Hydrology and Earth System Sciences, 4, *905–914* (1997) © EGS

Hydrology & Earth System Sciences

Interpacket diffusion in SAMP model for water and solute movement in unsaturated soil

John Ewen* and Greg M. O'Donnell

Water Resource Systems Research Laboratory, Department of Civil Engineering, University of Newcastle upon Tyne, Newcastle upon Tyne, NE1 7RU
* Author for correspondence
Tel. 0191 2227930. Fax 0191 2226669. E-mail John.Ewen@ncl.ac.uk

Abstract

SAMP (subsystems and moving packets) is a recently developed method for modelling preferential flow and solute movement in porous media, and for determining the fate of 'new' and 'old' water and solute when the new enters a region containing the old. In a SAMP model, the modelled region (e.g. the unsaturated zone) is divided into cells, and the pore space within each cell is divided into many (often 100 or more) subsystems. Packets of water, containing solute, move within and between the cells, from subsystem to subsystem, thus simulating the bulk movement of water and solute. A theory is developed here for representing molecular diffusion in the liquid phase of porewater as interpacket diffusion, and this theory is implemented in the SAMP 1 one-dimensional vertical-column model. The model is found to exhibit appropriate sensitivity to its parameters, and is successfully calibrated against existing laboratory breakthrough data for tritium movement in Glendale silty clay loam. The quality of fit achieved to the laboratory data is found to be significantly better when interpacket diffusion is simulated than when it is not. The main parameters for the model are those for the matric potential and unsaturated hydraulic conductivity functions, and the only parameter requiring calibration is the internal scale, which affects both interpacket diffusion and the way packets move within the soil. Theoretical and numerical comparisons show there are similarities between the internal scale and the coefficient for solute exchange between the dynamic region and dead-space in the two-region (mobile-immobile) model of van Genuchten and Wierenga (1976).

Introduction

The SAMP (subsystems and moving packets) approach to modelling the non-steady movement of water and solute in unsaturated porous media was developed recently by Ewen (1996ab; hereafter referred to as PA and PB). It was developed in response to the need for a new generation of models for simulating the complex non-equilibrium movements (e.g. preferential flow) which commonly take place in the unsaturated zone. SAMP models can be used to solve Richards' equation; to simulate advection and dispersion of solute in soil containing dead-space; to simulate preferential water and solute movement in soil containing macropores; and to determine the fate of 'new' and 'old' water and solute when the new enters a region containing the old.

In a SAMP model the modelled region (e.g. the unsaturated zone) is divided into cells, and the pore space within each cell is divided into many, often 100 or more, distinct independent thermodynamic subsystems. Discrete packets of water (which may contain solute) are moved from subsystem to subsystem, within and between the cells, and these movements simulate the effects of equilibrium and non-equilibrium movements of water and the advection and bulk dispersion of solute.

The parameters for a SAMP model are those for the matric potential and unsaturated hydraulic conductivity functions, as used with Richards' equation, plus a further parameter, the internal scale. The internal scale controls the mixing of old and new waters, and the degree to which non-equilibrium moisture states can be sustained in the soil. It has the symbol Λ.

Molecular diffusion in the liquid phase of pore moisture is not accounted for in the original SAMP theory. It is considered here, as part of a wider investigation of the nature of the internal scale. A theory is developed for interpacket diffusion, and this theory is incorporated in an upgraded version of the SAMP 1 one-dimensional vertical-column model. The upgraded model is then tested against existing laboratory data for breakthrough experiments involving the movement of tritium through columns of Glendale silty clay loam.

SAMP 1 Model

Full details of the basic SAMP theory are given in PA, where the theory is developed from first principles and the assumptions made are discussed. SAMP 1 models the movement of water and solute in a vertical column of plan area α and length β, which is divided into cells of plan area α and thickness $\delta\xi$. Each cell contains pore volume V ($V=\alpha\delta\xi p$, where p is the cell porosity), and each is divided into N subsystems, numbered 1 to N. Each subsystem in a given cell can be considered to be uniformly distributed within the cell. The low-numbered subsystems contain water which is strongly held by the soil matrix (i.e. the water contained in small pores and in thin layers adjacent to the walls of larger pores), and the high-numbered subsystems contain loosely held water (i.e. the bulk of the water in large pores in the matrix and in distinct macropores). The strength with which water is held in a given subsystem is related, through the SAMP theory, to the matric potential function for the medium contained in the cell. Each subsystem has the capacity to hold mass m (one packet) of porewater ($m=\rho V/N$, where ρ is the density of the porewater). At any given time, each subsystem must either hold a full packet or be completely dry. The moisture state of a cell can therefore be represented by an N-bit binary number, M. For example, if N is 8 and only subsystems 1, 2, 3, 6, and 7 are saturated (i.e. hold a packet) then $M = 01100111 = (1)_2(0)_2(1)_3$, where the subscripts indicate the number of times the digit in the corresponding brackets is repeated, and leading zeros are neglected.

The subsystems in a cell are independent, and each packet is a single conceptual entity. For a cell containing n packets, the volumetric moisture content, θ, is np/N and the internal equilibrium state is $(1)_n$. If a given cell is not in internal equilibrium, packets can move within it, from subsystem to subsystem, as a result of the spontaneous tendency for internal equilibrium to be approached (e.g. as happens when macropore water is absorbed by the matrix). In PA, this type of movement is called I-type movement. There are two other types: R-type and M-type. R-type movement involves packets moving from cell-to-cell under the action of gravity or spatial gradients in matric potential, and M-type movement involves movements in large, distinct macropores. The equations describing the movements of packets are based on Darcy's law, and give the probabilities of given moves taking place. The actual moves which will take place for a given cell for a given timestep are determined from these probabilities, using random numbers supplied by a random number generator. It is not practical to reproduce the probability equations here as there are too many of them (see PA).

SAMP 1 simulations proceed timestep-by-timestep, and for each timestep each cell is considered in turn: first the bottom cell, then the cell above it, etc., all the way up to the top cell. For each cell, the three types of movement are considered in turn, and all the necessary movements are completed before the next cell is considered. However, if a given cell is a boundary cell, injections and discharges of water packets are completed before the movements are considered, to ensure the boundary conditions are maintained.

Each packet of porewater has a fixed label-digit, e.g. '2', allowing it to carry information about the quality of the porewater. For example, if the internal state of a cell is $(1)_60(1)_{93}$, the solute state, S, might be the base-3 number $(2)_5102(1)_5(2)_{10}(1)_{77}$ showing that 16 of the packets (those labelled '2') have entered the column since the start of the simulation, and the other 83 (labelled '1') were present at the start of the simulation. The '2's can also be interpreted, if required, as indicating a given concentration of solute; and the movement, scattering, and retardation of contaminated (i.e. solute containing) packets interpreted as representing the effects of advection, dispersion, and dead-space. Many label-digits can be used simultaneously in one simulation, allowing the study of any combination of the effects of old and new, contaminated and uncontaminated, and of injections with time-varying concentrations of one or more chemical. A given label-digit can, of course, be associated with several properties; e.g. a cocktail of chemicals in new water.

Solute diffusion was not considered in the basic SAMP theory; it considered only the mechanical movement of solute associated directly with the movement of packets. To simulate solute diffusion requires that solute can move *between* packets. As a result, if solute diffusion is to be modelled, the solute state, S, will not be adequate as the sole simulation variable. In the new theory presented here, each subsystem will therefore be given, in addition to the usual label-digit, a concentration in the form of a base-10 number. (An alternative approach involving the extension of the concept of solute state, and which uses solute packets which move from water packet to water packet, is considered briefly in the discussion section.) There are, therefore, two simulation variables in the upgraded SAMP 1 model. The first is S (one base-3 number per cell) which now indicates only the source of the packets (old water, new water, etc.), and the second is the subsystem concentration (one base-10 number per subsystem), which equals the solute concentration in the packet currently contained in the subsystem, or zero if the subsystem is dry.

INTERNAL SCALE

One change is required to the existing SAMP theory in preparation for the development of the new theory for interpacket diffusion. It will be seen later that interpacket diffusion depends on a diffusion coefficient and the internal scale, A. The diffusion coefficient can be obtained from the literature (it is a property of the solute, not of the soil), and the internal scale can be calibrated against concentra-

tions measured in breakthrough experiments. The internal scale simultaneously controls three processes: I-type movement; R-type movement; and interpacket diffusion. It is therefore important that internal scale is used consistently across all three processes. Also, it is important to be strictly consistent with the physical interpretation of internal scale, so its numerical values can be analysed from a physical point of view.

In PA it was shown that the probability that an I-type movement will take place from subsystem i to subsystem j in the same cell is proportional to F_{ij}, where $F_{ij}=\Lambda k_i k_j/(k_i+k_j)$. The source of the conductivity ratio in this equation is the harmonic-mean conductivity for movement between the subsystems: $2k_ik_j/(k_i+k_j)$. In PA, the factor '2' from the harmonic mean was, for simplicity, assumed absorbed in Λ. However, to maintain the full physical nature of the definition of F_{ij}, it is redefined here as $F_{ij}=2\Lambda k_i k_j/(k_i+k_j)$.

Property and Simulation Data

In steady-flow pulse breakthrough experiments a steady flow with constant solute concentration is maintained through a column of soil for a long period. The solute concentration in the inlet water is then increased (or decreased) and kept high (or low) for a period of time before being returned to the original value; and the nature of the solute movement in the column is inferred from the effect this solute pulse has on the concentration in the water discharging from the column. The experimental data required for a SAMP 1 simulation of a steady-flow pulse breakthrough experiment involving downward vertical flow in an unsaturated soil are:

- c_o, c_p – inlet solute concentrations before and during the pulse (e.g. $kg\ m^{-3}$)
- D – diffusion coefficient for solute in porewater ($m^2\ s^{-1}$)
- $K(\theta)$ – unsaturated hydraulic conductivity of soil, as function of volumetric moisture content ($m\ s^{-1}$)
- l – length of column (m)
- p – porosity of soil (-)
- Q – flow rate ($m\ s^{-1}$)
- t_1, t_2 – time at start and end of pulse (s)
- θ_b – moisture content at base of column (-)
- $\psi(\theta)$ – matric potential of soil, as function of moisture content (m).

The hydraulic properties for each subsystem i in a given cell are the subsystem conductivity, k_i, and the total potential, Φ_i. These are determined in SAMP 1 from the soil hydraulic property functions and the elevation, z, measured at the centroid of the cell (PA Eqns 13 and 10):

$$k_i = K\left(\frac{ip}{N}\right) - K\left(\frac{(i-1)p}{N}\right) \quad (1 \le i \le N) \qquad (1)$$

and

$$\Phi_i = \psi_i + z \quad (1 \le i \le N \qquad (2)$$

where ψ_i, the subsystem potential, is given by PA (Eqn. 11):

$$\psi_i = N \int_{(i-1)/N}^{i/N} \psi d(\theta / p) \quad (1 \le i \le N) \qquad (3)$$

Full data sets giving the hydraulic property functions and breakthrough data for a (very nearly) conservative solute such as tritium are very rare. The two breakthrough experiments considered here are experiments 5–2 and 5–3 of van Genuchten and Wierenga (1977; hereafter referred to as VGW77). The soil is Glendale silty clay loam (GSCL), which has a porosity of 0.5, and the following property functions (Wierenga, 1977):

$$\begin{aligned}
\theta \le 0.325 \quad & \psi = -7.84 \times 10^{3} \exp(-31.3\theta) \quad (\mathrm{m}) \\
& K = 1.16 \times 10^{-20} \exp(92.1\theta) \quad (\mathrm{ms}^{-1}) \\
\theta > 0.325 \quad & \psi = -4.58 \times 10^{1} \exp(-15.5\theta) \quad (\mathrm{m}) \\
& K = 2.23 \times 10^{-11} \exp(26.3\theta) \quad (\mathrm{ms}^{-1}) \qquad (4)
\end{aligned}$$

The experiments involved the flow of a 0.01 N $CaCl_2$ solution through a 30 cm core of GSCL, subject to a pulse of tritium with an activity of 23,000 $cpm\ ml^{-1}$. In experiment 5–3 (all but one of the SAMP 1 simulations are for this experiment), the average volumetric moisture content in the core was maintained at 0.395 by a steady flow of 8.22 $cm\ day^{-1}$; the pore-volume time was 1.443 days, and the pulse lasted 2.763 pore-volumes. For experiment 5–2, the corresponding data are: 0.401; 16.6 $cm\ day^{-1}$; 0.725 days; 2.080 pore-volumes.

VGW77 ran 10-day batch equilibrium adsorption tests to determine the retardation factor for tritium in GSCL. These were unsuccessful, as the factor is very low. Adsorption is neglected in the SAMP 1 simulations.

Values of the coefficient for the self-diffusion of liquid water with tritium as a tracer are given by Wang *et al.* (1953). From their Figure 2, it can be estimated that $logD = -5.36 - 973/T$, where D has the units $m^2\ s^{-1}$ and T is the absolute temperature. Assuming the breakthrough experiments were run at 20°C, the appropriate value for D is, therefore, $2.1\times10^{-9}\ m^2\ s^{-1}$. The data on which the above equation is based were obtained using a capillary method, which in some ways recreates the effect of diffusion into and out of dead-end pores. Small capillaries between 19.4 and 47.4 mm in length and 0.187 and 0.220 mm^2 in area were filled with tritiated water, and their ends submerged for a period in a stirred bath of ordinary distilled water. The diffusion coefficients were determined based on the amount of tritium remaining in the capillaries on their removal from the bath.

SIMULATION DATA

The simulation data are:

N – number of subsystems per cell (–)
N_c – number of cells in column (–)
U – number of timesteps between diffusion calculations (–)
δt – timestep (s)
Λ – internal scale (m^{-2}).

The SAMP 1 model of the experiments is set up so that the top surface of the top cell corresponds to the top of the soil column, and the bottom surface of the bottom cell corresponds to the bottom of the soil column, so the thickness of each cell, $\delta\xi$, is β/N_c. Steady flow is simulated by injecting one packet of water into the top cell every w timesteps. (It is usual for the magnitude of δt to be chosen so that the time between injections [i.e. $p\delta\xi/(QN)$] is exactly $w\delta t$, and w is 2, 4, or 8.) Conditions at the bottom boundary are controlled by having a false cell (i.e. cell 0) below the bottom cell, and fixing the moisture content in this false cell. The initial condition in the column is set assuming that steady equilibrium flow is taking place. The 'standard' simulation (run 1, discussed later) has $N = 100$, $N_c = 30$, $U = 10$, $\delta t = 13.139$ s and $w = 4$.

In the breakthrough experiments, the pulse starts at time zero, so the tritium concentration in the inlet water rises at the beginning of the simulation, stays high for a period, then falls to zero. The packets in the column at the start of the simulations have label-digit '1' and concentration zero; during the pulse the injected packets have the label-digit '2' and concentration one; and the packets injected after the end of the pulse have label-digit '3' and concentration zero.

Interpacket Diffusion

The dispersion of solute in porous media is effected by both (molecular) diffusion and the mechanical mixing associated with water movement (Fried and Combarnous, 1971). When considering the bulk migration of solute, the direct contribution of diffusion can be significant, especially when the velocities of water movement are very low. This contribution has, for example, been considered by Millington and Shearer (1971) and Schaefer *et al.* (1995), who studied the relationship between the bulk migration rate, the liquid-phase diffusion coefficient, and resistances which describe the effect of the matrix. Diffusion has, however, a secondary effect on solute migration. It affects the concentrations at the pore-scale by allowing movements of solute between points in the liquid phase which are not strongly connected by water movement (e.g. diffusion into and out of dead-end pores). SAMP models are designed specifically to simulate the strongly coupled movements of water and solute, so bulk solute migration under diffusion is not a significant process in SAMP simulations, and it is the secondary effect of diffusion on solute migration which is of interest here.

In the SAMP approach each subsystem is assumed to be in direct contact with every subsystem in its cell. To model the secondary effect of diffusion on migration, it is therefore necessary to model the diffusional exchange of solute between each pair of subsystems in each cell. This exchange is similar in nature to the exchange between the dynamic region and dead-space in the two-region (mobile-immobile) model developed by Deans (1963), as used in the models of Coats and Smith (1964) and van Genuchten and Wierenga (1976). (Flühler *et al.*, 1996, used the term "lateral solute mixing" to describe these exchanges, and reviewed the modelling of lateral solute mixing for both two-region and multi-region models.) Setting SAMP to one side for a moment, and applying Deans (1963) approach to a cell in which there is a dynamic region and dead-space, the exchange rate, q ($kg\ s^{-1}$), from the dynamic region to dead-space is given by:

$$q = \frac{V}{p}\alpha_0(c - c^*) \tag{5}$$

where V/p is the total volume of soil in the cell, c and c^* are the concentrations in the dynamic region and dead-space, respectively, and α_0 (s^{-1}) is an exchange coefficient. This can be viewed as a finite-difference analogue of Fick's law; say the general concentration in the porewater is C, and there are two finite-difference cells, with nodal concentrations c and c^*, then:

$$q = -AD\frac{\partial C}{\partial x} \cong \frac{AD}{\delta x}(c - c^*) \tag{6}$$

where A is the effective area for diffusional exchange, D the coefficient for solute diffusion in porewater, and δx the distance between the nodes.

Fick's law of diffusion is analogous to Darcy's law, and the coefficient for liquid-phase diffusion, D ($m^2\ s^{-1}$), will be treated is the SAMP theory in an analogous manner to the unsaturated hydraulic conductivity (Eqn. 1): the subsystem diffusion coefficient, for all subsystems, will therefore be pD/N, where the porosity, p, accounts for the presence of the matrix. Using a finite-difference analogue of Fick's law, assuming both subsystems i and j in the same cell are saturated, the rate of diffusion from subsystem i to subsystem j is given by:

$$q = A\frac{pD}{N}\frac{(c_i - c_j)}{\delta\chi} \tag{7}$$

where, in this case, A is the effective area of contact between the packets, c_i the concentration in subsystem i, and $\delta\chi$ the average distance over which diffusion takes place. The volume of each packet is V/N, so the resulting change in concentration in subsystem j over period δt is $q\delta t/(V/N)$, giving:

$$\delta c_j = N\delta t\Lambda\frac{pD}{N}(c_i - c_j) \tag{8}$$

Table 1. Breakthrough simulations run using SAMP 1.

Run	Expt.	$Log_{10}\Lambda$	$D\times10^9$	N	N_C	U	RMSD
1	5–3	*3.55*	2.1	100	30	10	0.043
2	5–3	*3.69*	2.1	50	30	10	0.041
3	5–3	*3.29*	2.1	200	30	10	0.044
4	5–3	*3.45*	2.1	100	60	10	0.041
5	5–3	*3.64*	*2.86*	100	30	10	0.041
6	5–3	*3.55*	2.1	100	30	1	0.042
7	5–3	*13.68*	0	100	30	10	0.110
8	5–3	10.68	0	100	30	10	0.170
9	5–3	16.68	0	100	30	10	0.167
10	5–3	3.55	0.021	100	30	10	0.419
11	5–3	3.55	0.21	100	30	10	0.245
12	5–3	3.55	21.0	100	30	10	0.116
13	5–3	3.55	210.0	100	30	10	0.144
14	5–2	*3.77*	2.1	100	30	10	0.058
15	5–3	1,. . .,5	2.1	100	30	10	see Fig 3

where Λ is the internal scale ($=A/V\delta\chi$). The form of this equation is similar to that for the probability for I-type movement from subsystem i to subsystem j (derived from Darcy's law): from PA Eqns 20–22, if both subsystems are saturated, the probability equation can be written in the form:

$$\varepsilon_{ij}^{I} = N\delta t F_{ij}(\psi_i - \psi_j) = N\delta t \Lambda \frac{2k_i k_j}{k_i + k_j}(\psi_i - \psi_j) \quad (9)$$

UPGRADING SAMP 1

The theory above was implemented in the SAMP 1 model for a single solute. A concentration is allocated to each packet when it first appears in the simulation, and the concentration in a given packet changes subsequently only as the result of interpacket diffusion. When a given packet moves from one subsystem to another it carries its solute with it, and each saturated subsystem takes on, as its subsystem concentration, the concentration of the packet it contains; dry subsystems have zero concentration. The computer processing times for SAMP 1 are increased considerably by the computation of interpacket diffusion, so the interpacket diffusion calculations are carried out only once every U timesteps (typically $U = 10$).

In the calculation of interpacket diffusion for a given cell, each pair of subsystems is considered in turn. The calculations start with the highest-numbered subsystem, and involve its pairing with the second highest subsystem, the third highest subsystem, etc. Calculations are then carried out for pairs based on the second highest subsystem, then the third highest, etc. In total, $(N - 1) + (N - 2) + (N - 3) + . . . + 1$ pairs are considered (= 4950 for $N = 100$). When a given pair is considered, the concentrations of both subsystems are updated before the next pair is considered. (The results were found to be insensitive to both the order of calculation and the updating procedure used.) Based on Eqn. 8, the equation for calculating the change in concentration for subsystem pair i,j is:

$$\delta c_j = -\delta c_i = M_i M_j U \delta t \Lambda p D(c_i - c_j) \quad (10)$$

where M_i is 1 if subsystems i is saturated, and zero otherwise.

Results

Table 1 gives details of the breakthrough simulations carried out using SAMP 1. The values in italics in this table are calibrated values, found by minimising the root-mean-square-difference (RMSD) between the SAMP 1 breakthrough concentration and the measured concentration. (The SAMP 1 breakthrough concentration is found by averaging the concentration in the packets leaving the column; typically each average is calculated over a few hundred packets.) For runs 1–4, 6, 7 and 14, the optimisation routine BRENT from Press *et al.* (1986) was used to calibrate Λ, and for run 5, the routine AMOEBA, also from Press *et al.* (1986), was used to simultaneously calibrate Λ and D. The quality of fit of the SAMP 1 results to the laboratory measurements can be seen in Figs. 1 and 2.

For runs 1–6, RMSD lies in the very narrow range 0.041–0.044, showing that the quality of fit is insensitive to N, N_c, U, and to whether Λ is calibrated for fixed D, or Λ and D are calibrated simultaneously. There is no interpacket diffusion in runs 7–9, and by comparing the RMSD values and breakthrough concentrations (Fig. 1) for runs 1 and 7 it can be seen that there is a substantial improvement in the quality of fit when interpacket diffusion is simulated.

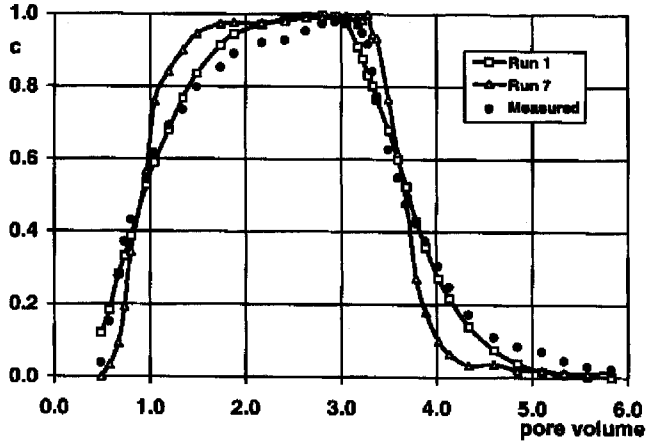

Fig. 1. *Simulated and measured breakthrough concentrations for experiment 5–3.*

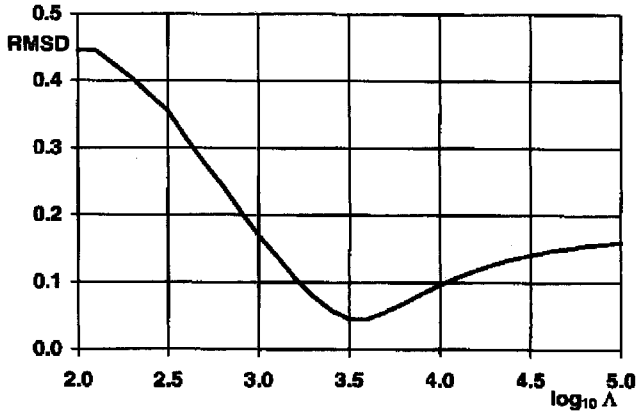

Fig. 3. *RMSD for a range of internal scale, for the parameter set for run 1.*

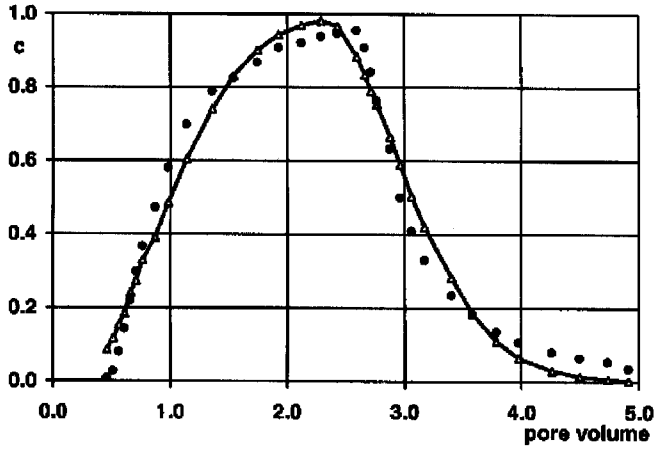

Fig. 2. *Simulated (line) and measured (circles) breakthrough concentrations for experiment 5–2 (run 14).*

Runs 8–13 and 15 show the sensitivity to Λ and D. The sensitivity to Λ is best illustrated by run 15 (Fig. 3) which involved 41 simulations with $log_{10}\Lambda$ set to 1.0, 1.1, 1.2, etc. (the results for $log_{10}\Lambda$ less than 2 are not plotted in Fig. 3 since I-type movement is so greatly restricted at these low values of Λ that a steady flow cannot be maintained).

The calibrated value for Λ varies strongly with D. $Log_{10}\Lambda$ is 3.55 for $D = 2.1 \times 10^{-9}\ m^2\ s^{-1}$ (run 1) and 13.68 for $D = 0$ (run 7). The main reason for this is that, as discussed below, both Λ and D affect the timing and shape of the breakthrough curve. Fig. 4 shows the distribution of the label-digits '1' and '2' after one pore-volume of time in run 1. The new water, label-digit '2', is confined mainly to a band, approximately covering subsystem numbers 50 to 80. The lower-numbered subsystems do, however, play a significant role in solute movement, as can be seen in the concentration distribution shown in the lower part of Fig. 4; solute gets into these subsystems mainly by interpacket diffusion. The results for run 7 ($log_{10}\Lambda = 13.68$; $D = 0$) would look quite different if plotted alongside Fig. 4. The band containing label-digit '2' would be much wider and less fragmented, and the subsystems with label-digit '1' would have zero concentration. Despite this, runs 1 and 7, have similar breakthrough curves. If the pulse for experiment 5–3 simply moved through the full saturated portion of the pore space without delay or dispersion, the breakthrough curve would be a perfect (square) pulse, rising to unit concentration after one pore-volume of time, and falling back to zero concentration after 3.763 pore-volumes. As can be seen in Fig. 1, however, both runs 1 and 7 have slightly early breakthrough, reaching a concentration of 0.5 after approximately 0.9 pore-volumes, and both curves have a rounded shape, which shows the effect of dispersion within the column. For run 1, one of the main controls on timing and dispersion is the strength of interpacket diffusion: the stronger the diffusion, the greater the mixing in the cells, the later the breakthrough, and, in general, the more rounded the breakthrough curve. In contrast, in run 7 there is no interpacket diffusion ($D = 0$), and the sole controlling parameter on timing and dispersion is Λ: the greater is Λ, the wider the band of label-digit '2', the greater the delay in breakthrough, and the greater the dispersion as a result of the natural I and R-type movement within the band.

Fig. 5 shows the distribution of the label-digits and concentration for run 1, after four pore-volumes of time. The tritium injection pulse ended after 2.736 pore-volumes, and the subsystems with label-digit '3' contain packets injected since that time. It can be seen that much of the original water (label-digit '1') is still in the column, especially in subsystems 1–50, and there are also some packets with label-digit '2', which were injected during the pulse.

Both Figs. 4 and 5 show that interpacket diffusion, with $D = 2.1 \times 10^{-9}\ m^2\ s^{-1}$, is not perfectly efficient at spreading the solute within a cell. For example, for cell 5 in

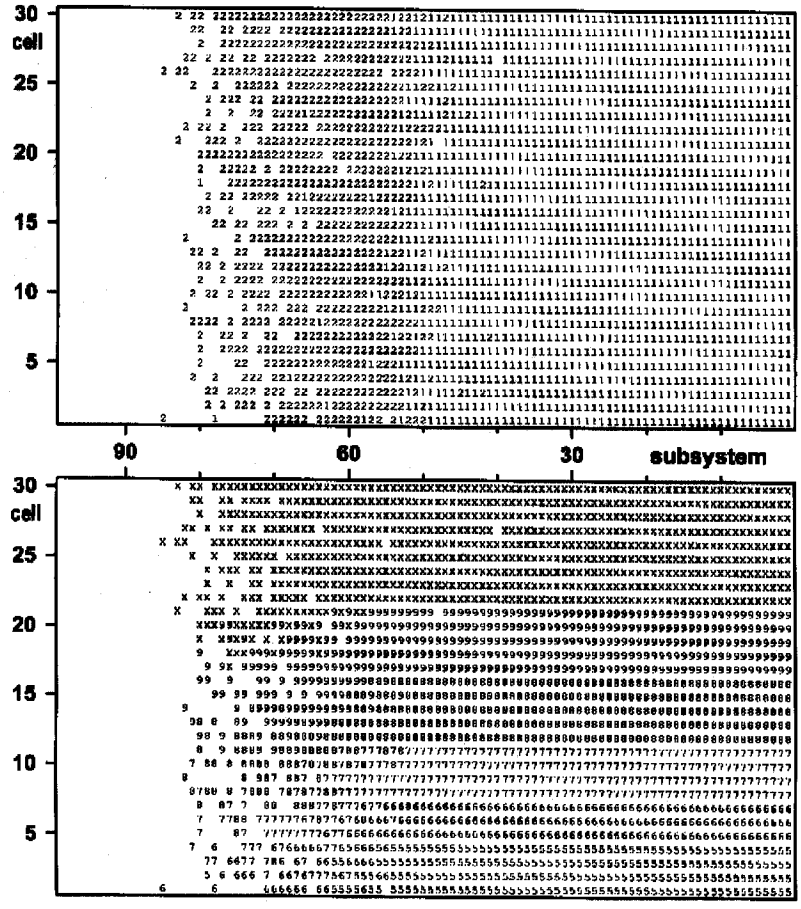

Fig. 4. *Moisture and solute distributions after one pore-volume (1.443 days) of time for run 1. Top section shows label-digits ('1' for old water and '2' for new); bottom section shows subsystem concentration multiplied by 10 and rounded to the nearest whole number ('X' represents 10).*

Fig, 5, the concentration in the low-numbered subsystems is around 0.3, which is substantially greater than the concentration in the high-numbered subsystems (0.1–0.2).

The runs for experiment 5–3 with $D = 2.1 \times 10^{-9}$ m^2 s^{-1} all have similar calibrated values of Λ. In considering the differences between the calibrated Λs for the different runs it is important to recognise there is some variability between simulations as a result of the stochastic nature of the model. For example, during the calibration process which gave the value for Λ for run 1, the BRENT routine had difficulty in finding an exact minimum: Fig. 6 shows the RMSD values calculated during the final stages of the calibration. Based on this figure and Fig. 3, it is reasonable to say that the calibrated $log_{10}\Lambda$ for run 1 is 3.55 ± 0.02.

For run 6 ($U = 1$) the calibrated Λ is the same as for run 1 ($U = 10$). It therefore appears that reducing the computation run times by carrying out interpacket diffusion calculations only every 10th timestep, rather than every timestep, does not affect the quality of the results obtained.

The effect on Λ of increasing the number of cells used by a factor of two can be seen by comparing run 1 (30 cells) and run 4 (60 cells). The calibrated Λ for run 1 is 3.55 ± 0.02, and for run 4, 3.45 ± 0.02, so there is only a small difference (-0.10 ± 0.04) between these. Larger differences arise when the number of subsystems is varied from 100 (run 1) by a factor of two: 0.14 ± 0.04 for 50 subsystems (run 2) and -0.26 ± 0.04 for 200 subsystems (run 3).

Discussion

It is clear from the results of the SAMP 1 simulations that the inclusion of interpacket diffusion improves the quality of the simulations. However the cost of including interpacket diffusion is very high: a typical simulation of experiment 5–3 involves over 0.7 billion calculations of the diffusional exchange between pairs of subsystems, and takes around 20 minutes of processing time on a single processor on a medium-performance UNIX workstation.

The strength of the movement of solute under interpacket diffusion can be considered in terms of the rate of decay of the difference in concentration between an isolated pair of saturated subsystems. Say the isolated sub-

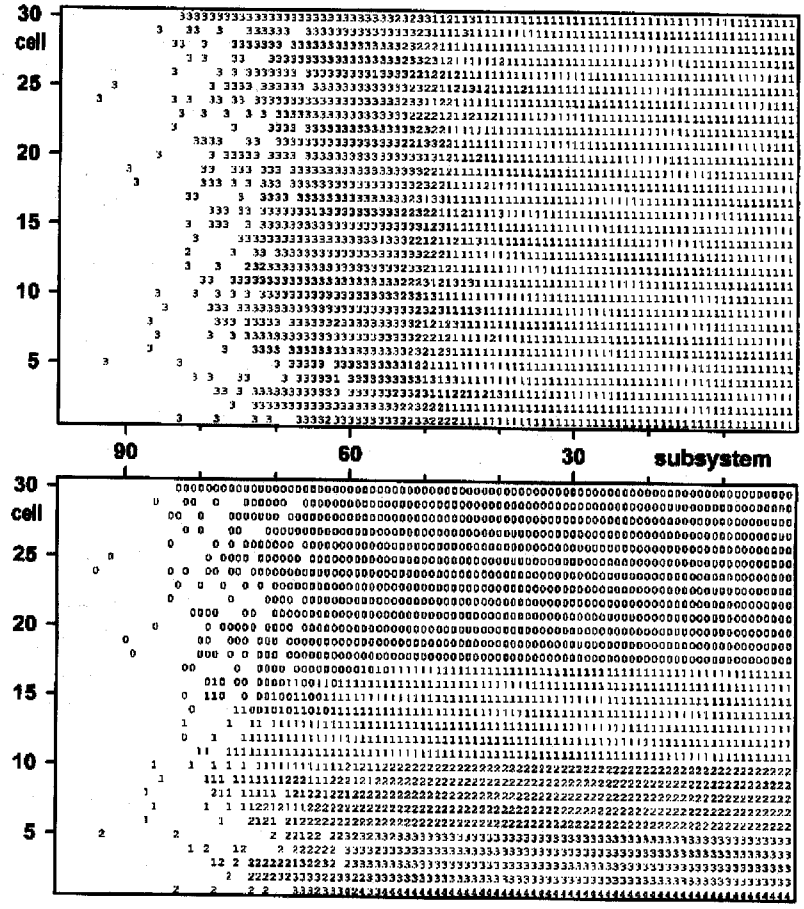

Fig. 5. *Moisture and solute distributions after four pore-volumes of time (5.772 days) for run 1. Top section shows label-digits ('1' for old water; '2' for water injected during the tritium pulse; '3' for water injected since the end of the pulse); bottom section shows subsystem concentration multiplied by 10 and rounded to the nearest whole number.*

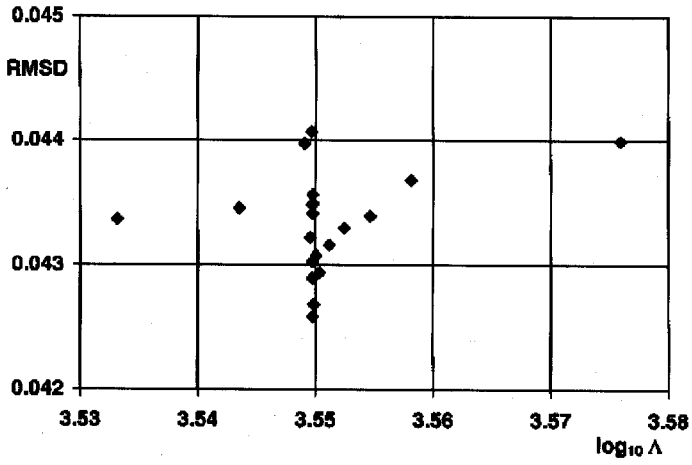

Fig. 6. *RMSD for simulations run during the late stages of the calibration of internal scale, Λ, for the parameter set for run 1.*

systems are given the numbers 1 and 2, and their initial concentrations are c_{01} and c_{02}, respectively. Converting Eqn. 10 to an ordinary differential equation and solving it gives the concentration in subsystem 1 after time t: $c_1 = 0.5[c_{01} + c_{02} - (c_{02} - c_{01})exp(-2\Lambda pDt)]$. The time for the difference in concentration between the two subsystems to fall to half its initial value is therefore $-ln(0.5)/(2\Lambda pD)$, which for run 1 gives 25.84 hr (= 0.746 pore-volumes). This shows that interpacket diffusion is a slow process relative to the rate of injection of packets (1 packet per 52.556 s in run 1), and that quite large values can be used for the effective timestep, $U\delta t$, for the calculation of interpacket diffusion ($U\delta t$ = 131.39 s for run 1).

Based on the evidence above that interpacket diffusion is a slow process, a new, computationally-efficient method is being developed for simulating interpacket diffusion. This method is more in the spirit of the SAMP approach than the method developed here, and uses packets of solute which move from subsystem to subsystem. A state variable, similar to S, records the (integer) number of solute packets in each subsystem, and the states change

only as a result of the movement of solute packets. The main complication with this approach arises in its extension to modelling soil conditions in which there is both diffusion and adsorption of solute to the matrix.

VGW77 fitted two models to their breakthrough data: the convection-dispersion equation (they based this on Lindstrom *et al.*, 1967), and their own (now widely used) two-region model (van Genuchten and Wierenga, 1976). Based on the simulation results in VGW77, for experiment 5–3 the convection-dispersion equation gives an RMSD = 0.155, and the two-region model an RMSD = 0.011. SAMP 1 (RMSD = 0.043) therefore gives a much better fit than the convection-dispersion equation, but a poorer fit than the two-region model (which has four calibrated parameters, compared to one in SAMP 1).

By definition, $\Lambda = A/V\delta\chi$, where A is the area of contact between each pair of subsystems, V the pore volume of the cell, and $\delta\chi$ the effective distance over which I-type movement and interpacket diffusion takes place. Before trying to interpret the physical meaning of the calibrated value for Λ it is important to be aware of the difficult task Λ performs as the sole calibrated parameter. Its effect on interpacket diffusion and I-type movement is relatively straightforward and physical (Eqns 8 and 9). However, its effect on R-type movement is not straightforward. The probability, ε^R, of an R-type move taking place during period δt from a given cell (cell A) to the cell below (cell B) is independent of Λ, but the probability of an R-type move taking place from a given subsystem i in cell A to a given subsystem j in cell B does depend on Λ. From PA Eqns 33–35:

$$\varepsilon^R_{ij} = \varepsilon^R e_{ij} \Big/ \sum_{r=1}^{am} \sum_{s=1}^{bm} e_{rs} \qquad (11)$$

where

$$e_{ij} = L^{AB}_{ij} k_j \sum_{u=1}^{am} M^A_u \left(\frac{1}{\gamma F_{iu}} + \frac{V\delta\xi}{2\alpha k_u} \right)^{-1} \qquad (12)$$

where $L^{AB}{}_{ij}$ is zero unless subsystem i in cell A is saturated and subsystem j in cell B is dry, in which case it is one; am is the highest-numbered saturated subsystem in cell A, bm the highest-numbered saturated subsystem in cell B, and $M^A{}_u$ is one if subsystem u in cell A is saturated, and zero otherwise. (When comparing the results here with those in PB it should be noted that F has be redefined, and γ is $N\delta t$ in PB but is unity here and in PA.) In effect, the probability that it is subsystem i which releases a packet when there is an R-type move from cell A to cell B depends on F, and hence on Λ [since $F_{ij} = 2\Lambda k_i k_j/(k_i + k_j)$.]. Eqns 11 and 12 are less physical than the equations which link Λ to interpacket diffusion and I-type movement, and, as discussed in PA, some arbitrary choices were (necessarily) made in their derivation.

For run 1, $log_{10}\Lambda = 3.55$, so $\Lambda = 3{,}548\ m^{-2}$. In PA an equation was derived for Λ for packet movement between aggregates and a coarse interaggregate material: $\Lambda = 12(1-f)/(a^2 p)$, where fraction f of the soil comprises interaggregate materials, and the aggregates are cubes with side length a. There are n aggregates per cell [$n = (1-f)V/(a^3 p)$], and Λ was assumed equal to the ratio of the total surface area ($6na^2$) of the aggregates in the cell to the product of the pore volume (V) and the distance from the surface to the centre of an aggregate ($a/2$). To get an indication of the physical scale of the calibrated value of Λ for run 1, if $f = 0$ and $p = 0.5$, the calculated side length, a, for $\Lambda = 3{,}548\ m^{-2}$ is 8.22 cm. This is large, and shows that the connections between the subsystems are quite weak, which is a conclusion supported by Figs. 4 and 5: the weak connections result in non-equilibrium flow, as shown by the fragmented nature of the distribution of water packets in subsystems 60–100.

It should be expected that Λ is insensitive to V, provided V is large enough to cover a representative sample of the pore structures seen within the soil. This seems to be borne out by the close agreement between the calibrated values for Λ for runs 1 and 4 (run 4 has packets half the size of those in run 1). The area A (and perhaps $\delta\chi$), on the other hand, should be expected to vary with the number of subsystems, N, in the cell, so Λ should vary with N. Theoretical bounds for the relationship between Λ and N can be estimated in a simple fashion. Say the porewater behaves as a very large number ($>>N$) of subvolumes with linear dimension a; then $A \propto N^{-1}$ and $\delta\chi \propto a \propto 1$, so $\Lambda = A/(V\delta\chi) \propto N^{-1}$. Taking the other extreme view, say each subsystem contains a volume with typical linear dimension a; then $a^3 \propto N^{-1}$, $A \propto a^2 \propto N^{-2/3}$ and $\delta\chi \propto a \propto N^{-1/3}$, so $\Lambda \propto N^{-1/3}$. For run 1, $log_{10}\Lambda = 3.55$ and $N = 100$; the expected range for $log_{10}\Lambda$ when $N = 50$ is, therefore, 3.65–3.85, which spans the calibrated value, 3.69 (run 2). For $N = 200$ the range is 3.25–3.45, which also spans the calibrated value, 3.29 (run 3). The calibrated value for Λ therefore behaves as expected: decreasing with N, such that it is proportional to a value lying between N^{-1} and $N^{-1/3}$.

It is possible to compare the calibrated values for Λ against the values for α_0, the exchange coefficient VGW77 found on calibrating their two-region model. Comparing Eqns 5 and 7, if $N = 2$, $\alpha_0 = \Lambda p^2 D/2$. For experiment 5–3 ($log_{10}\Lambda = 3.55$) this gives $\alpha_0 = 0.93 \times 10^{-6}\ s^{-1}$. The value from VGW77 is $3.13 \times 10^{-6}\ s^{-1}$. For experiment 5–2 the corresponding figures are $1.55 \times 10^{-6}\ s^{-1}$ and $3.59 \times 10^{-6}\ s^{-1}$. For both experiments, the calculated and calibrated values for α_0 are similar. However, it is not appropriate to take this analysis further since there are significant differences between a two-subsystem SAMP model and the two-region model (which, for example, has regions which are unequal in size).

Conclusions

Theory has been developed for within-cell interpacket

diffusion in SAMP models, and this theory has been implemented in the SAMP 1 one-dimensional vertical-column model. SAMP 1 was successfully calibrated against existing laboratory tritium-breakthrough data for columns of Glendale silty clay loam. The main parameter controlling interpacket diffusion is the coefficient for solute diffusion in porewater. This is a property of the solute, not the soil, and for tritium diffusion in water a value of 2.1 $\times$ 10^{-9} m^2 s^{-1} was obtained from the literature. The sole calibrated parameter is the internal scale. This affects interpacket diffusion, and the way packets move through the soil. Calibration was carried out with and without interpacket diffusion, and the quality of the fit between the SAMP 1 results and the laboratory data found to be substantially better with interpacket diffusion. Many simulations were run, and SAMP 1 was found to exhibit appropriate sensitivity to the number of cells and subsystems used, and to the diffusion coefficient.

The similarity between interpacket diffusion and the exchange of solute between the dynamic region and dead-space in a two-region (mobile-immobile) model was investigated, and theoretical and numerical comparisons suggest there is a link between internal scale and the exchange parameter in the two-region model of van Genuchten and Wierenga (1976).

References

Coats, K.H. and Smith, B.D. (1964) Dead-end pore volume and dispersion in porous media. *Soc. Pet. Eng. J.* **4**: 73–84.

Deans, H.A. (1963) A mathematical model for dispersion in the direction of flow in porous media. *Trans. AIME* **228**: 49–52.

Ewen, J. (1996a) 'SAMP' model for water and solute movement in unsaturated porous media involving thermodynamic subsystems and moving packets: 1. Theory. *J. Hydrol.* **182**: 175–194.

Ewen, J. (1996b) 'SAMP' model for water and solute movement in unsaturated porous media involving thermodynamic subsystems and moving packets: 2. Design and application. *J. Hydrol.* **182**: 195–207.

Flühler, H., Durner, W. and Flury, M. (1996) Lateral solute mixing processes – a key for understanding field-scale transport of water and solutes. *Geoderma* **70**: 165–183.

Fried, J.J. and Combarnous, M.A. (1971) Dispersion in porous media. *Adv. Hydrosci.* **7**: 169–282.

Lindstrom, F.T., Haque, R., Freed, V.H. and Boersma, L. (1967) Theory on the movement of some herbicides in soils. *Environ. Sci. Technol.* **1**: 561–565.

Millington, R.J. and Shearer, R.C. (1971) Diffusion in aggregated porous media. *Soil Sci.* **111**: 372–378.

Press, W.H., Flannery, B.P., Teukolsky, S.A. and Vetterling, W.T. (1986) *Numerical Recipes.* Cambridge University Press, Cambridge, UK.

Schaefer, C.E., Arands, R.R., van der Sloot, H.A. and Kosson, D.S. (1995) Prediction and experimental validation of liquid-phase diffusion resistance in unsaturated soils. *J. Contam. Hydrol.* **20**: 145–166.

van Genuchten, M.Th. and Wierenga, P.J. (1976) Mass transfer studies in sorbing porous media: I. Analytical solutions. *Soil Sci. Soc. Am. J.* **40**: 473–480.

van Genuchten, M.Th. and Wierenga, P.J. (1977) Mass transfer studies in sorbing porous media: II. Experimental evaluation with tritium (^3H_2O). *Soil Sci. Soc. Am. J.* **41**: 272–278.

Wang, J.H., Robinson, C.V. and Edelman, I.S. (1953) Self-diffusion and structure of liquid water. III. Measurement of the self-diffusion of liquid water with H^2, H^3 and O^{18} as tracers. *J. Am. Chem. Soc.* **75**: 466–470.

Wierenga, P.J. (1977) Solute distribution profiles computed with steady-state and transient water movement models. *Soil Sci. Soc. Am. J.* **41**: 1050–1055.